RSC Advances

ROYAL SOCIETY OF CHEMISTRY

www.rsc.org/advances

Cite this: DOI: 10.1039/c0xx00000x

www.rsc.org/xxxxxx

ARTICLE TYPE

Plasmon-Induced Decarboxylation of Mercaptobenzoic Acid on Nanoparticles Film Monitored by Surface-Enhanced Raman Spectroscopy

Yi Zong‡, Qinghua Guo‡, Minmin Xu, Yaxian Yuan*, Renao Gu, Jianlin Yao*

Received (in XXX, XXX) Xth XXXXXXXXX 20XX, Accepted Xth XXXXXXXXX 20XX
DOI: 10.1039/b000000x

Surface plasmon played an important role in the surface catalysis reaction, and thus the tuning of plasmon on metal nanostructures and the extension of plasmon induced surface catalysis reaction have been of the attractive issues. Au nanoparticles monolayer film was fabricated by the assembling of Au nanoparticles at liquid/air interface held with numerous "hot spots" for the strong surface plasmon coupling. A facile approach was developed to achieve the decarboxylation reaction by appropriate surface plasmon on the Au nanoparticles monolayer film surface, and surface enhanced Raman spectroscopy (SERS) has been developed as the sensitive tool for in situ monitoring the plasmon induced surface reaction. The effect of power and wavelength of the laser, solution pH on the decarboxylation reaction was investigated. With the laser illumination, *para*-mercaptobenzoic acid (PMBA) was transferred to thiophenol (TP) in which the decarboxylation was enhanced with the increase of laser power and illumination time. The results revealed that the carboxylate groups of the adsorbed PMBA molecules were removed to produce TP which still adsorbed on Au surfaces. The solution pH values exhibited significant influence on the decarboxylation reaction. In the air and neutral solution, decarboxylation proceeded in a slow rate to transfer from PMBA to TP, while it was absent in acidic solution. The deprotonated carboxylate group accelerated the decarboxylation for producing TP with a fast rate in alkaline solution. As a comparison, the similar plasmon driven decarboxylation reaction was observed on the Ag nanoparticles monolayer film surface. It suggested that the transformation on Au nanoparticles film surface from PMBA to TP molecules under the laser illumination was associated with a surface-catalyzed reaction driven by local surface plasmon.

Introduction

Decarboxylation reaction has attracted considerable interest in organic synthesis. It is well known that removal of carboxylate groups opens versatile connection points for construction of carbon frameworks, for example, the decarboxylative cross-coupling reaction for the large scale synthesis of interesting organic molecules.[1-4] In addition, carboxylic acid derivatives used as the reactants are inexpensive, ubiquitous and easy to handle, meanwhile the stoichiometric byproduct of CO_2 is nontoxic and easily removed.[5, 6] Although decarboxylation of highly activated carboxylic acids occurred reasonably well even in the absence of a catalyst, the release of CO_2 from simple aromatic carboxylic acids was much difficult to accomplish.[7] In recent years, the development of metal-catalyzed decarboxylation reactions provided the effective approach to the deeper insights into the process of decarboxylation.[7-10] However, the reported methods of decarboxylation still remained difficulties which essentially required usage of toxic metals and harsh organic bases. In a word, severe experimental conditions might be required for the extrusion of CO_2 from carboxylic acids.[4, 6] Consequently, the facile and metal-free strategy is highly desired to accomplish the decarboxylation reaction. So far, there have been great efforts to devise more favorable decarboxylation conditions with various improvements. For example, Sinha et al. developed a metal-free decarboxylation reaction by using ionic liquids as clean catalyst cum solvent.[11]

Recently, the emergence of new technologies provided a facile approach to cover the long-standing problems in the metal-catalyzed decarboxylation reaction. For example, the nanoparticles have become the key subjects in the field of catalysis due to the unique effect at nanometer scale, such as the large ratio of surface atoms, and the size and morphology of metal particles become one of the critical factors on catalytic reactivity. However, the metal nanoparticles played the similar role by comparing with the metal-complex catalysts, in which the aggregation of the metal nanoparticles restricted to develop their advantages well. Actually, besides catalytic activities, the metal nanoparticles have attracted considerable attention due to the tunable optical properties depended on the size, shape and metal catalogues. For instance, Au nanoparticles exhibited excellent surface enhanced optical effect originated from the surface

plasmon resonance. So far, surface plasmon has been already investigated by many research groups across various fields. The plasmonic heating and plasmon-induced charge are advantageous when coupled to Au nanoparticles as catalyst and noninvasive heat therapy. Furthermore, the illumination on the Au nanoparticles at the plasmon resonance frequency contributed the giant plasmonic charge and heating, and it was used successfully to drive catalytic reactions. By integrating strongly plasmonic and catalytic nanoparticles, significant enhancements in the catalytic activity were achieved, including conversion of CO to CO_2,[12, 13] reduction of CO_2,[14-16] degradation of pesticides,[17, 18] water splitting,[19, 20] dissociation of H_2,[21] water treatment,[22] and so on.[23-25] Most importantly, the enhanced electric fields produced near plasmon resonant metallic nanoparticles have been utilized in the surface-enhanced Raman spectroscopy (SERS), yielding enhancement factors as high as 14 folders which make it possible to reach single molecule detection. Therefore, the plasmonic nanostructures promised to be a breakthrough for driving photon-assisted processes at nanometer scale level and allowed to in situ probe the mechanism of the relevant processes at molecular level. So far, *in situ* monitoring of plasmon-driven chemical reactions has received a good deal of attentions, particularly for the N-N coupling reaction on metal nanoparticles. Ren and his coworkers reported the first experimental and theoretical investigation of the plasmon assisted catalytic coupling reaction of *p,p′*-dimercaptoazobenzene (DMAB) produced from para-aminothiophenol (PATP).[26] They also investigated the catalytic oxidation which was mainly contributed to the activation of oxygen through the surface plasmon on metal nanoparticles.[27] Sun *et al.* reported the direct experimental and theoretical evidences of the surface-catalyzed transformation from PATP to DMAB assisted by local surface plasmons.[28] Then a range of investigations have also supported the findings revealed by SERS spectroscopy.[29-32]

Although recent advances have opened up possibilities for the novel applications of plasmon on chemical reactions, the decarboxylation reaction was rarely associated with that.[33-36] Wagner et al. reported the near-UV illumination of o-acetylphenyl- and o-benzoylphenylacetic acids, producing the efficient decarboxylation.[37] Beckert and his coworker developed the laser photolysis of amino acid solution.[38] The time resolved Fourier transform electron paramagnetic resonance (FT-EPR) spectroscopy was employed to monitor the photolysis processes, indicating oxidation of amino acids through a one-electron transfer followed by a rapid decarboxylation. By the illumination of intense laser pulses at 532 nm, the selective decarboxylation of two aspartic acids was observed in the vicinity of the retinal chromphore by the mass spectroscopy.[39] Wan et al. reported the photodecarboxylation of benzoyl-substituted biphenylacetic acids and photo-retro-aldol reaction of related compounds in aqueous solution.[40] They also proposed the mechanism of photo-assisted decarboxylation reaction.

Para-mercaptobenzoic acid (PMBA) has been used as an important SERS probe molecule owing to its strong interaction with noble metals mostly through S-metal bond and thus contributed enhanced SERS signals.[41] Generally, the probe molecule was inert on the metal surface under the laser illumination. Michota *et al.* have reported that PMBA molecules underwent decarboxylation when assembling on a Ag electrode and they considered that the roughness of Ag electrode surfaces contributed to the main factor influencing decarboxylation.[42] Unfortunately, the partial decarboxylation was observed and further exploring on the reaction was absent. Therefore, it was worthy to further investigate the decarboxylation of PMBA to obtain the high transformation efficiency and the deeper insight into the reaction mechanism.

Here, a uniform Au nanoparticle monolayer film was assembled to generate the reasonable surface plasmon resonance. A systematical investigation of PMBA adsorbed on Au film surfaces has been revealed by SERS. And the similar experiments were performed on Ag nanoparticle film as comparison. The plasmonic catalytic decarboxylation was explored by using different laser powers, wavelengths and solution pH values. A preliminary mechanism on the decarboxylation reaction was proposed.

Experimental Section

Chemicals and Materials

Chloroauric acid ($HAuCl_4 \cdot 4H_2O$), Silver nitrate ($AgNO_3$), Polyvinylpyrrolidone (PVP), Hydroxylamine hydrochloride ($NH_2OH \cdot HCl$), Trisodium citrate ($Na_3C_6H_5O_7 \cdot 2H_2O$), Sodium hydroxide (NaOH), Hydrochloric acid (HCl) and ethanol (C_2H_5OH) were purchased from Sinopharm Group Co. Ltd. (China), while 4-mercaptobenzoic acid (PMBA, $C_7H_6O_2S$) was purchased from TCI. Si(111) wafer with a resistance of 0.025 Ω·cm was used as the substrate for collecting the Au or Ag nanoparticle film. All solution was prepared by Milli-Q water. Different pH solutions at pH 2, 5, 10 and 12 were prepared by aqueous solutions of 0.01 M HCl and 0.01 M NaOH, respectively.

Synthesis of Au and Ag nanoparticles

Aqueous Au sol was prepared following the recipes of Frens.[43] Initially, 1 mL of 1% $HAuCl_4 \cdot 4H_2O$ aqueous solution was dissolved with 100 mL water, and the solution was heated to a boil under vigorous stirring. Subsequently a solution of 1% sodium citrate (2 mL) was added quickly. When the solution color turned to wine-red, it was kept in boiling for 15 min and then cooled down. Thus, Au nanoparticles with 15 nm diameter were obtained as seeds. Larger size of Au nanoparticles were synthesized by the procedure of Tian.[44] Under the presence of PVP and sodium citrate, 25 mM $NH_2OH \cdot HCl$ was added into the seeds solution. Then constant concentration of $HAuCl_4$ was added to above mixed solution under vigorous stirring. Finally, the Au nanoparticles with the diameter of about 30 nm were obtained (as shown in Fig. 1).

The Ag sol was prepared according to the method of Lee and Meisel.[45] Firstly, $AgNO_3$ (10 mg) was dissolved in water (100 mL) and the solution was brought to a boil. Then, 1 mL 1% sodium citrate was quickly added under vigorous stirring. After the solution was kept boiling for 1 h, a colloidal solution containing Ag nanoparticles with a diameter of 80 nm and a small quantity of Ag nanorods was obtained (the SEM image of Ag nanoparticles was presented in supporting information).

Assembly of Au and Ag nanoparticle monolayer film

The metal nanoparticle monolayer film was obtained from a two-phase interface assembling approach. The as-prepared Au nanoparticles with PVP as stabilizer floated on the solution surface (air-liquid interface), while the Ag nanoparticles were assembled at liquid-liquid interface. A clean oxidized Si wafer was immersed into the two phase interface with a tilt angle, and then lifted in a constant speed to transfer the nanoparticle monolayer film onto the Si wafer as a plasmon generated substrate. The Si wafer attached with metal nanoparticle film was then immersed in an ethanol solution containing 1 mM PMBA for 2 hours and then was washed with ethanol twice and Milli-Q water to remove the physically adsorbed PMBA prior to the laser illumination and SERS measurements.

Instruments

Raman spectra were recorded with a confocal microprobe Raman instrument (HR800, Jobin Yvon, France) under the illumination of 632.8 nm and 785 nm excitation lines. The Raman spectrometer was equipped with a microscope with 50× long-distance objective. The width of silt and the size of the pinhole were 100 μm and 400 μm, respectively. However, the laser power was changed from 5 mW to 2.5 mW, 1.3 mW and 0.5 mW.

Results and discussion

Fig. 1a presented the schematic diagram of Au nanoparticles monolayer film modified with PMBA molecules. The compact package of Au nanoparticles generated numerous junctions at the adjacent nanoparticles, so called as "hot spots". Generally, the strong electric field covered the "hot spots" owing to the coupling effect of the localized surface plasmon (LSP) between two nanoparticles.[46] As a consequence, the Raman scattering intensity of the molecules located in the "hot spots" increased dramatically, and heat effect originated from the surface plasmon was also applied onto the molecules, resulting in a plasmonic catalytic chemical reaction. Fig. 1b presented the SERS spectra of PMBA adsorbed on an Au nanoparticle monolayer film. The strong bands at about 1077 cm^{-1} and 1588 cm^{-1} were assigned to ν_{12} and ν_{8a} aromatic ring vibrations, respectively.[47] The SERS spectra of PMBA adsorbed on the Au nanoparticle film with a different feature was incidentally observed (Fig. 1c). One could be clearly noticed that two new bands were detected at about 1003 cm^{-1} and 1026 cm^{-1} accompanied with a shoulder peak of 1577 cm^{-1}. It suggested the generation of new specie which adsorbed on the Au nanoparticles together with the PMBA molecules. The SERS spectra showed essentially identical spectral characteristics with that of thiophenol (TP) molecules adsorbed on Au metal surfaces (as shown in Fig. 1d), which convincingly evidenced the production of TP from PMBA by decarboxylation under the catalytic effect of Au nanoparticles.[48] By carefully comparing the relative intensities and the band frequencies of the spectra presented in Fig. 1 c and d, one could find that the spectral feature contained the mixture of PMBA and TP molecules. Actually, the ambient conditions and excitation line exhibited significant influence on the plasmonic catalyzed reaction.

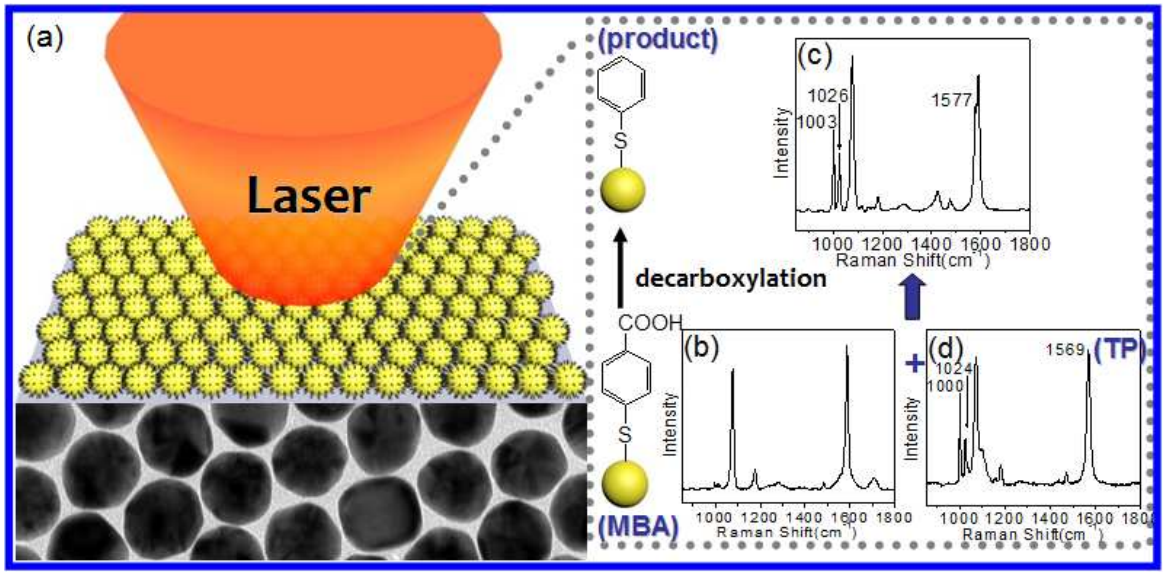

Fig. 1 (a) Schematic diagram of the plasmon-induced surface catalyzed decarboxylation, the SERS spectra (b) and (c) collected before and after decarboxylation reaction of PMBA, (d) SERS spectra of TP adsorbed on Au nanoparticles monolayer film.

Fig. 2 presented the time-dependent SERS spectra of PMBA adsorbed onto the Au nanoparticle films in air by different excitation lines. According to Fig. 2a and 2c, the time dependent SERS spectra of PMBA absorbed on the Au film in air were obtained by using 632.8 nm and 785 nm illumination as the excitation line, respectively. The duration of SERS measurements was 100 seconds and the spectra were both recorded every 10 seconds. It should be pointed out that the intensity of bands at

1588 cm^{-1} decreased significantly and it became weaker than that of 1077 cm^{-1} by using 785 nm as the excitation line, while the intensities of above two main bands were comparable for 632.8 nm as excitation line. It was mainly contributed to the different enhancement and the efficiency of CCD detector and grating under the different excitation line.

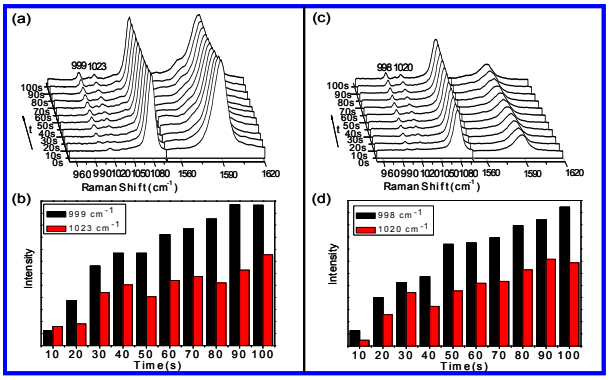

Fig. 2 (a) Time dependent SERS spectra of PMBA adsorbed on Au nanoparticles monolayer film in air using 632.8 nm laser as the excitation line, (b) histogram of time dependent peak intensity of the new bands at 999 and 1023 cm^{-1} under above condition, (c) time dependent SERS spectra of PMBA on Au nanoparticles monolayer film in air using 785 nm laser as the excitation line, (d) histogram of time dependent peak intensity of the new bands at 998 and 1020 cm^{-1} under above condition.

For example, for the band at 1588 cm^{-1} originated from the excitation line of 785 nm, the photon energy was located at the lower quantum efficiency of CCD detector, and thus the signal decreased correspondingly, while for the excitation line of 632.8 nm, its photon energy was located at the higher quantum efficiency of the detector. Two new bands at about 999 and 1023 cm^{-1} corresponding to the adsorbed TP could be weakly identified and the intensity of these bands seemed to change with the illumination duration. In order to descript clearly, the illumination time dependent bands intensities of new bands were presented in Fig. 2b and 2d. At the initial stage, the intensity of the bands of TP increased steadily. After 50 seconds, there was no distinct increase in the intensity and a shoulder band accompanied with the 1589 cm^{-1} band was appeared. It indicated that only a few PMBA molecules underwent the plasmonic induced decarboxylation in the air. Due to the surface plasmon resonance on Au nanoparticle film excited by the laser with the wide range of wavelength (from red light to near IR region), the plasmon catalyzed reaction occurred by the present two excitation lines. Therefore, the very similar change in the spectral feature was observed. However, the lower fraction of the decarboxylated molecule on the surface resulted in the poor potential practical application. Thus, it was worthy to control the environments to obtain the high surface reaction yield.

Normally, the carboxylate group was removed through the byproduct of CO_2. Therefore, it was reasonable to assume that the deprotonated carboxylate group (COO^-) was considered as the appropriate format for the decarboxylation reaction. In the present case, the solution pH of 2, 5, 7, 10 and 12 were used to investigate the capabilities of decarboxylation, and the SERS spectra in the solution pH 2, 7 and 12 were presented in Fig. 3 together with the SERS spectrum from the air. SERS spectra in pH 5 and pH 10 solutions were shown in supporting information.. The SERS spectra detected immediately in aqueous solution at pH 2 exhibited the characteristic SERS spectrum of PMBA adsorbed on the Au nanoparticle film. One could conclude that the plasmonic induced decarboxylation reaction was absent in acidic solution. With the increase in the pH values, the decarboxylation was occurred partially, and the very similar spectral feature to that in the air was observed in the pH=7 solution. Fig. 3d presented the spectrum of PMBA on an Au film measured in the solution with pH12. Two new bands at 1003 and 1026 cm^{-1} accompanied by stronger band at 1577 cm^{-1} consistent with adsorbed TP were distinctly observed, which confirmed experimentally that the surface plasmonic catalyzed transformation from PMBA to TP occurred, i.e. the decarboxylation reaction was favourable in the high pH solution. A similar change with the spectral characteristic has also been observed on Ag nanoparticle monolayer film (as shown in Fig. 3e). Three new bands corresponding to adsorbed TP appeared which indicated the PMBA molecules underwent decarboxylation reaction to generate TP. It was coincident with the investigation by Michota *et al.* on Ag electrode measured in the alkaline solution of PMBA.[42] Based on the above mentioned fact, it was reasonable to deduce that the decarboxylation processes was induced by the surface plasmon in alkaline solution. By carefully analyzing the spectrum after laser illumination, one could find that the surface spectral contained the molecules of TP and PMBA together, no intermediate species was detected during the decarboxylation. It revealed that removal of the deprotonated carboxylate group occurred in a very rapid rate and simply routine induced by the surface plasmon.

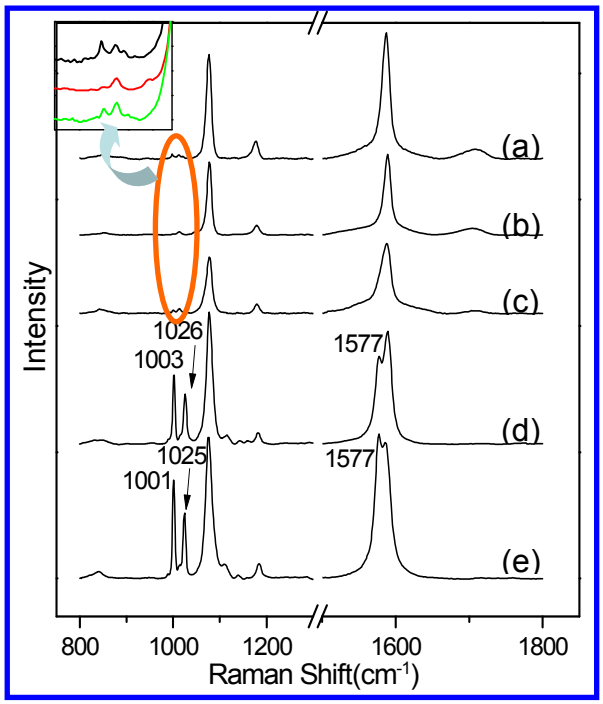

Fig.3 SERS spectra of PMBA on an Au nanoparticle film measured in air (a), in aqueous solution at pH 2 (b), pH 7(c)and pH12(d), SERS spectra of PMBA on an Ag film taken at pH 12 (e) by using 632.8 nm as the excitation line. Inserted figure was

the magnification in a narrow spectral region of spectra (a), (b), and (c)

By comparing the spectral feature presented in Fig. 3d (on Au substrate) and e (on Ag substrate) carefully, one could find the relative intensity of bands at 1577 cm^{-1} and 1588 cm^{-1} was dependent on the nature of substrates, in which the former band was contributed to the decarboxylation product while the latter was originated from adsorbed PMBA. It could be served as the criteria to determine the conversion rate of PMBA to TP. the relative intensity of $I_{1577/1588}$ was about 0.75 on the Au substrate, while on Ag substrate, $I_{1577/1588}$=1.07. It indicated that Ag substrate exhibited higher catalytic efficiency for the plasmon induced decarboxylation reaction under the illumination of 633 nm laser.

The laser power dependent decarboxylation of PMBA on Au nanoparticle film was investigated in aqueous solution at pH 12 by using power of 0.5 mW, 1.3 mW, 2.5 mW, 5 mW respectively (as shown in Fig. 4). Interestingly, three new bands at 1001, 1025 and 1577 cm^{-1} assigned to TP appeared when the laser power was high enough (5 mW) and the intensities of new bands increased obviously with the increasing of laser power. As seen from Fig. 4c and 4d, the new bands exhibited much obviously at 2.5 mW and 5 mW. Thus, it should be pointed out that higher laser power was also more favourable for the occurrence of the decarboxylation of PMBA molecules on Au nanoparticle film surface. Actually, the previous investigation revealed that the plasmon could decay to assemble hot electrons on the nanoparticles surface.[21,25,49] In the present case, the Au nanoparticle monolayer film generated numerous "hot spots" for the surface plasmon coupling to enhance plasmon resonance, thus the sufficient hot electrons could be assembled in the "hot spots", resulting in the catalysis of molecule adsorbed therein. The laser power played the dual functions to drive the surface chemical reaction, i.e. generation of sufficient hot electrons to induce the decarboxylation and local heating effect to accelerate the reaction. The former function was dominated, while the latter was assisted in the plasmon catalyzed decarboxylation.

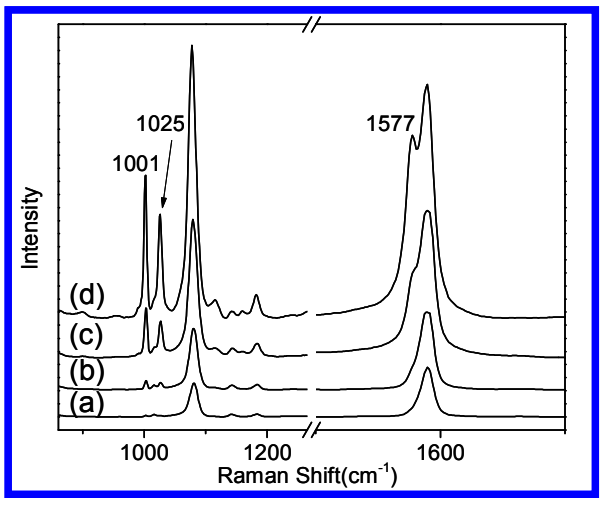

Fig. 4 SERS spectra of PMBA on Au film measured at the same point immediately in aqueous solution at pH 12 using (a) 0.5 mW, (b) 1.3 mW, (c) 2.5 mW, (d) 5 mW respectively as the laser power.

In order to resolve the surface decarboxylation procedure, the time dependent SERS spectra were in situ monitored at pH 12 by using 785 nm illumination (as shown in Fig. 5). Three new bands at 998 cm^{-1}, 1022 cm^{-1} and 1572 cm^{-1} assigned to TP molecule were observed and increased obviously in intensities with the prolonged illumination duration. The conflicting relationship was observed between the intensities of the bands of 1572 cm^{-1} and 1586 cm^{-1} which were assigned to TP and PMBA respectively, i.e. the former increased in intensity followed with the decrease of the latter. It indicated that the molecule of PMBA was transferred to TP which still adsorbed onto surface. It should be pointed out that the SERS intensity of the band at 1073 cm^{-1} was contributed by the TP and PMBA together. Interestingly, the SERS intensity of the band at 1073 cm^{-1} became stronger with the increase of the illumination time. In the present case, the PMBA was attached onto the Au nanoparticle film surface and the physical adsorption of PMBA was removed. As a consequence, the monolayer of PMBA was covered onto the film surface. There were no additional free PMBA molecules to supply the reactant molecule during the laser illumination. Therefore, the increase in the intensity of the band at 1073 cm^{-1} mainly due to the following two reasons: i) the stronger enhancement effect on the TP than PMBA, ii) the removal of carboxylate group resulted in the decrease of steric hindrance, and thus the coverage of TP was higher than that of PMBA. The additional TP was originated from the mobilization of PMBA to the "hot spots" driven by laser illumination. Fig. 5b presented the SERS intensity-time profile of TP and PMBA. The initial intensity of PMBA and the intensity of the product detected at 100 second were used to normalize the SERS intensities detected at different period of the surface plasmon catalyzed reaction. One could find that the intensities of new bands increased fast at the beginning and then tended to steady increase after 60 sec. Generally, the strong coupling of surface plasmon in the "hot spots" generated giant electromagnetic field which enhanced the Raman scattering signal of molecules therein. Therefore, the PMBA molecules located in "hot spots" were undergone the plasmon driven decarboxylation reaction firstly, and the SERS signal of the plasmonic catalyzed product changed in a fast rate. After laser illumination of 60 seconds, the PMBA molecules outside of "hot spots" began to undergo the decarboxylation with a relative slow rate. Moreover, the molecules located in the "hot spots" contributed the dominant SERS intensity. Although the strong thermal effect originated from the focused laser was applied on the "hot spots" in air, the decarboxylation proceeded at a slow rate due to the lack of the deprotonated carboxylate group. The present experiment was performed in aqueous solution in which the "hot spots" surrounding was water and thermal effect should be weakening dramatically.[46] Therefore, the surface plasmon played the critical role in the decarboxylation processes. The very similar laser-induced behaviour has also been reported with PATP, the appearance of "b_2 mode" peaks was possibly attributed to the transformation from PATP to DMAB. It was mainly due to the surface reaction induced significantly by the local heating effect and surface plasmon of nanoparticles especially when the excitation line was in agreement with the LSPR bands of the substrate.[29] Based on the above experimental fact, one could assume that the transformation on Au nanoparticles film surface

from PMBA to TP molecules was associated with a surface-catalyzed reaction driven by local surface plasmon.

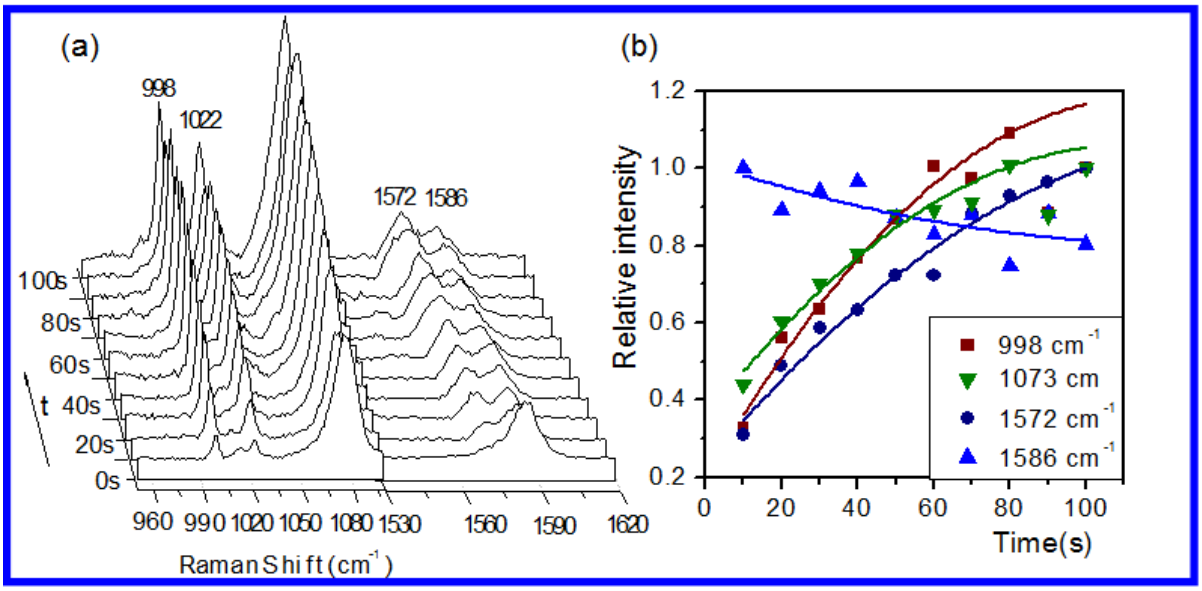

Fig.5 (a) Time dependent SERS spectra of PMBA on Au nanoparticles film measured at the same point in aqueous solution at pH 12 using 5 mW as the laser power and 785 nm illumination as the excitation line, (b) Time dependent relative intensity of the new bands

Conclusions

The Au nanoparticle monolayer film was fabricated by the assembling of Au nanoparticles at liquid/air interface which hold numerous "hot spots" for the strong surface plasmon coupling. A facile approach for the decarboxylation reaction was developed on the Au nanoparticles monolayer film surface under the laser illumination. The effect of power and wavelength of the laser, solution pH on the decarboxylation reaction was investigated. After the laser illumination, three new bands corresponding well with TP appeared and their intensity enhanced with the increase of laser power and illumination time, and very similar surface reaction was observed by different excitation lines of 632.8 nm and 785 nm which excited the surface plasmon on the Au nanoparticles film. It revealed that the carboxyl group of the adsorbed PMBA molecules was removed to produce TP which still adsorbed on Au surfaces. The solution pH values exhibited significant influence on the decarboxylation reaction. In the air and neutral solution, the decarboxylation proceeded in a very slow rate and was not completely transferred from PMBA to TP, while it was absent in acidic solution. The deprotonation of carboxylate group accelerated the decarboxylation for producing TP in alkaline solution. As a comparison, the similar plasmon driven decarboxylation reaction was observed on the Ag nanoparticle monolayer film surface. The results suggested that the transformation on Au nanoparticle film surface from PMBA to TP molecules under the laser illumination was associated with a surface-catalyzed reaction driven by local surface plasmon. Our results revealed that the laser played the critical functions for generating the strong surface plasmon coupling to enhance the SERS signal and to induce the plasmon catalyzed decarboxylation, and SERS could be developed as a powerful tool to in situ monitor the surface reaction processes. Although more issues about this methodology must be addressed, including the transformation yield, the generality, the capability for the C-C coupling reaction, and the recycling of the substrate with appropriate surface plasmon, the preliminary results have shown it opens a facile routine for the decarboxylation and the corresponding construction of new carbon frameworks and complex organic molecules for the practical application.

Acknowledgments

The authors gratefully acknowledge the financial support from the Nature Science Foundation of China (21073128, 21033007, 21173155) and the National Instrumentation Program (2011YQ031240402). The partial financial support from the project of scientific and technologic infrastructure of Suzhou (SZS201207), and a project funded by the Priority Academic Program Development of Jiangsu Higher Education Institutions (PAPD) are gratefully acknowledged.

Notes and references

[a] *College of Chemistry, Chemical Engineering and Materials Science, Soochow University, Suzhou, 215123, China. E-mail :yuanyaxian@suda.edu.cn, jlyao@suda.edu.cn*

† Electronic Supplementary Information (ESI) available: [details of any supplementary information available should be included here]. See DOI: 10.1039/b000000x/

‡ Equal contribution

1 A. F. Shepard, N. R. Winslow and J. R. Johnson, *J. Am. Chem. Soc.*, 1930, **52**, 2083-2090.
2 M. Nilsson, *Acta Chem. Scand.*, 1966, **20**, 423-426.
3 A. G. Myers, D. Tanaka and M. R. Mannion, *J. Am. Chem. Soc.*, 2002, **124**, 11250-11251.
4 L. J. Goossen, G. Deng and L.M. Levy, *Science*, 2006, **313**, 662-664.
5 J. D. Weaver, A. Recio III, A. J. Grenning and J. A. Tunge, *Chem. Rev.*, 2011, **111**, 1846-1913.
6 N. Rodríguez and L. J. Goossen, *Chem. Soc. Rev.*, 2011, **40**, 5030-5048.
7 L. J. Gooßen, W. R. Thiel, N. Rodríguez, C. Linder and B. Melzer, *Adv. Synth. Catal.*, 2007, **349**, 2241-2246.
8 L. J. Goossen, C. Linder, N. Rodriguez, P. P. Lange and A. Fromm, *Chem. Commun.*, 2009, 7173-7175.

9 J. S. Dickstein, C. A. Mulrooney, E. M. O'Brien, B. J. Morgan and M. C. Kozlowski, *Org. Lett.*, 2007, **9**, 2441-2444.
10 L. Q. Xue, W. P. Su and Z. Y. Lin, *Dalton Trans.*, 2011, **40**, 11926-11936.
11 A. Sharma, R. Kumar, N. Sharma, V. Kumar and A. K. Sinha, *Adv. Synth. Catal.*, 2008, **350**, 2910-2920.
12 E. M. Larsson, C. Langhammer, I. Zorić and B. Kasemo, *Science*, 2009, **326**, 1091-1094.
13 W. H. Hung, M. Aykol, D. Valley, W. Hou and S. B. Cronin, *Nano lett.*, 2010, **10**, 1314-1318.
14 W. B. Hou, W. H. Hung, P. Pavaskar, A. Goeppert, M. Aykol and S. B. Cronin, *ACS Catal.*, 2011, **1**, 929-936.
15 C. An, J. Wang, W. Jiang, M. Zhang, X. Ming, S. Wang and Q. Zhang, *Nanoscale*, 2012, **4**, 5646-5650.
16 M. J. Kale, T. Avanesian and P. Christopher, *ACS Catal.*, 2014, **4**, 116-128.
17 J. F. Guo, B. W. Ma, A. Y. Yin, K. N. Fan and W. L. Dai, *Appl. Catal., B,* 2011, **101**, 580-586.
18 D. M. Fouad and M. B. Mohamed, *Plasmonics*, 2013, **8**, 937-941.
19 H. Gao, C. Liu, H. E. Jeong and P. Yang, *ACS Nano*, 2012, **6**, 234-240.
20 Z. W. Liu, W. B. Hou, P. Pavaskar, M. Aykol and S. B. Cronin, *Nano lett.*, 2011, **11**, 1111-1116.
21 S. Mukherjee, F. Libisch, N. Large, O. Neumann, L. V. Brown, J. Cheng, J. B. Lassiter, E. A. Carter, P. Nordlander and N. J. Halas, *Nano lett.*, 2013, **13**, 240-247.
22 H. F. Qian, L. A. Pretzer, J. C. Velazquez, Z. Zhao and M. S. Wong, *J. Chem. Technol. Biotechnol.*, 2013, **88**, 735-741.
23 J. R. Adleman, D. A. Boyd, D. G. Goodwin and D. Psaltis, *Nano lett.*, 2009, **9**, 4417-4423.
24 S. Linic, P. Christopher, H. Xin and A. Marimuthu, *Acc. Chem. Res.*, 2013, **46**, 1890-1899.
25 A. Giugni, B. Torre, A. Toma, M. Francardi, M. Malerba, A. Alabastri, R. Proietti Zaccaria, M. I. Stockman and E. Di Fabrizio, *Nat. Nanotechnol.*, 2013, **8**, 845-852.
26 Y. F. Huang, H. P. Zhu, G. K. Liu, D. Y. Wu, B. Ren and Z. Q. Tian, *J. Am. Chem. Soc.*, 2010, **132**, 9244-9246.
27 Y. F. Huang, M. Zhang, L. B. Zhao, J. M. Feng, D. Y. Wu, B. Ren and Z. Q. Tian, *Angew. Chem., Int. Ed.*, 2014, **53**, 2353-2357.
28 Y. Fang, Y. Li, H. Xu and M. T. Sun, *Langmuir*, 2010, **26**, 7737-7746.
29 D. Y. Wu, X. M. Liu, Y. F. Huang, B. Ren, X. Xu and Z. Q. Tian, *J. Phys. Chem. C*, 2009, **113**, 18212-18222.
30 M. T. Sun, Y. X. Hou, Z. P. Li, L. W. Liu and H. X. Xu, *Plasmonics*, 2011, **6**, 681-687.
31 M. T. Sun and H. X. Xu, *Small*, 2012, **8**, 2777-2786.
32 Y. F. Huang, D. Y. Wu, H. P. Zhu, L. B. Zhao, G. K. Liu, B. Ren and Z. Q. Tian, *Phys. Chem. Chem. Phys.*, 2012, **14**, 8485-8497.
33 Y. Tsuboi, R. Shimizu, T. Shoji and N. Kitamura, *J. Am. Chem. Soc.*, 2009, **131**, 12623-12627.
34. K. Ueno, S. Juodkazis, T. Shibuya, Y. Yokota, V. Mizeikis, K. Sasaki and H. Misawa, *J. Am. Chem. Soc.*, 2008, **130**, 6928-6929.
35 C. Hubert, A. Rumyantseva, G. Lerondel, J. Grand, S. Kostcheev, L. Billot, A. Vial, R. Bachelot, P. Royer, S. H. Chang, S. K. Gray, G. P. Wiederrecht and G. C. Schatz, *Nano lett.*, 2005, **5**, 615-619.
36 C. J. Chen and R. M. Osgood, *Phys. Rev. Lett.*, 1983, **50**, 1705-1708.
37 M. Sobczak and P. J. Wagner, *Org. Lett.*, 2002, **4**, 379-382.
38 J.-M. Lü, L. M. Wu, J. Geimer and D. Beckert, *Phys. Chem. Chem. Phys.*, 2001, **3**, 2053-2058.
39 M. Imhof, D. Rhinow, U. Linne and N. Hampp, *J. Phys. Chem. Lett.*, 2012, **3**, 2991-2994.
40 M. S. Xu, M. Lukeman and P. Wan, *J. Photochem. Photobiol. A*, 2009, **204**, 52-62.
41 S. J. Li, R. A. Gu, *Acta Chim. Sinica*, 2004, **62**, 2118-2122.
42 A. Michota and J. Bukowska, *J. Raman Spectrosc.*, 2003, **34**, 21-25.
43 G. Frens, *Nat. Phys. Sci.*, 1973, **241**, 20-22.
44 P. P. Fang, J. F. Li, Z. L. Yang, L. M. Li, B. Ren and Z. Q. Tian, *J. Raman Spectrosc.*, 2008, **39**, 1679-1687.
45 P. C. Lee and D. Meisel, *J. Phys. Chem.*, 1982, **86**, 3391-3395.
46 G. K. Liu, J. Hu, P. C. Zheng, G. L. Shen, J. H. Jiang, R. Q. Yu, Y. Cui and B. Ren, *J. Phys. Chem. C,* 2008, **112**, 6499-6508.
47 H. Park, S. B. Lee, K. Kim and M. S. Kim, *J. Phys. Chem.*, 1990, **94**, 7576-7580.
48 K. T. Carron and L. G. Hurley, *J. Phys. Chem.*, 1991, **95**, 9979-9984.
49 Z. L. Zhang, L. Chen, M. T. Sun, P. P. Ruan, H. R. Zheng and H. X. Xu, *Nanoscale*, 2013, **5**, 3249-3252.